

PERFORMANCE EVALUATION FOR HALL EFFECT SENSORS BASED ON CONFIGURATION

Tobechukwu D. Nwabueze¹, Ross Zamoski¹, and Tony Schmitz^{1,2}

¹Mechanical, Aerospace, and Biomedical Engineering

University of Tennessee, Knoxville

Knoxville, TN 37996, USA

²Manufacturing Demonstration Facility

Oak Ridge National Laboratory

Oak Ridge, TN 37830, USA

INTRODUCTION

The intent of Industry 4.0 is to integrate digital technologies into production environments. This requires sensors that have low cost with high sensitivity and bandwidth. In this project, affordable sensors for displacement measurements during manufacturing processes are evaluated. Displacement can be measured using eddy current sensors, capacitive sensors, and laser interferometry, for example. In many cases, however, the cost is too high for broad implementation. In this work, Hall effect sensors, which can be implemented at low cost, are evaluated to determine the sensitivity and range. Hall effect sensors detect the flux density from a magnet field and output a signal proportional to the relative displacement between the magnet and sensor. Hall effect sensors are available with a range of magnetic field sensitivities, so tests are performed in this study with different Hall effect sensor-magnet combinations to determine the corresponding sensitivity and range. Optical stages are used to perform the tests, where an air bearing stage is used to set the gap between the sensor and magnet and the voltage is recorded.

LITERATURE REVIEW

Different designs and combinations of Hall effect sensors have been used for various linear and angular displacement measurements. Six single-axis Hall effect sensors were attached to the stator with a ring-shaped permanent magnet mounted on the rotor as the magnetic flux source [1]. Hall effect sensors were implemented on dual-axial motion control of a magnetic levitation system. Two sensors were used for each axis of motion (x , y , and z) in a magnetically guided robot's working space. The magnetic sensitivity of the TLE4990 Infineon Hall effect sensor was 22 mV/mT [2]. A system made up of three Hall effect sensors and six permanent magnets was designed to measure displacement along three

degrees of freedom. The system recorded a sensitivity of about 1.54 V/mm over a 5 mm height [3]. Another system made up of two Hall effect sensors and a magnet between them was designed for linear displacement measurements with a sensitivity of 0.35 V/mm over a linear range of 2.98 mm [4]. A machine learning-enabled Hall effect system for monitoring building vibrations was reported. Seismic events and the count of steps made by people walking in a public building were detected [5].

RESEARCH DESCRIPTION

The research objective is to evaluate Hall effect sensor displacement measurement performance, including sensitivity and range. Different sensor-magnet pair configurations are selected for evaluation and sensitivity measurement results are provided. The two configurations tested in this study are shown in Figs. 1 (axial motion) and 2 (lateral motion). The test setup is shown in Fig. 3.

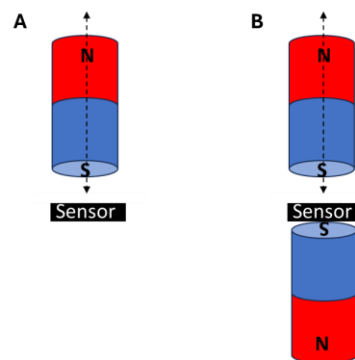


FIGURE 1. Two axial sensor-magnet configurations. (A) a unipolar sensor is placed in front of the south pole of a magnet and moved along the sensor axis (dashed line). (B) The south pole of a magnet is attached to the back of a unipolar sensor (i.e., back biased), while another magnet is moved along the sensor axis.

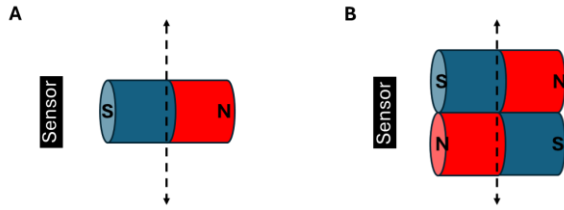


FIGURE 2. Two lateral sensor-magnet configurations. (A) A single magnet is moved laterally past a bipolar sensor. (B) Two magnets with opposite poles are moved laterally past a bipolar sensor.

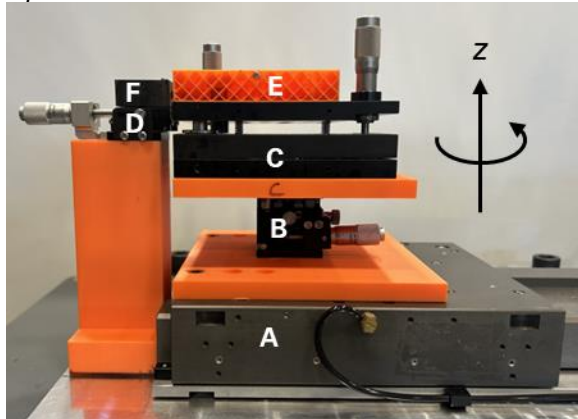


FIGURE 3. Experimental setup (axial motion) with the sensor holder (F) on the left and the magnet holder (E) on the right. The stages are labeled A (Aerotech ABL 10100-LT automated air bearing stage to provide known displacements), B (Edmund Optics vertical manual stage), C (Newport model 37 manual stage rotating around x, y, and z axes), and D (Edmund Optics horizontal manual stage).

To test and compare changes in sensitivity values with changes in small misalignments of the sensor-magnet configurations during the axial and lateral motions, the Newport model 37 manual rotating stage was rotated around z-axis and the Edmund Optics vertical manual stage was translated along z-axis as shown in Figs. 4 and 5. The rotation and translation misalignments were tested in positive and negative increments from the nominal alignment. The rotation and translation were determined by measuring the manual stage motions with a structured light scanner and calibrating the micrometer graduations.

RESULTS

Testing was performed to determine the sensitivity and linear range for each sensor-magnet combination. This was completed by positioning the magnet relative to the sensor

using an air bearing stage. The air bearing stage has an encoder with high resolution and low uncertainty, so its position was assumed to be correct and enabled the sensor-magnet sensitivity and linear range to be determined from the voltage-position data.

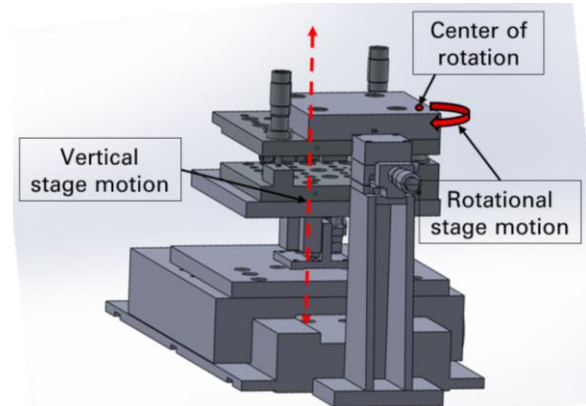


FIGURE 4. Vertical and rotational stage motions along and around z-axis for the axial configuration.

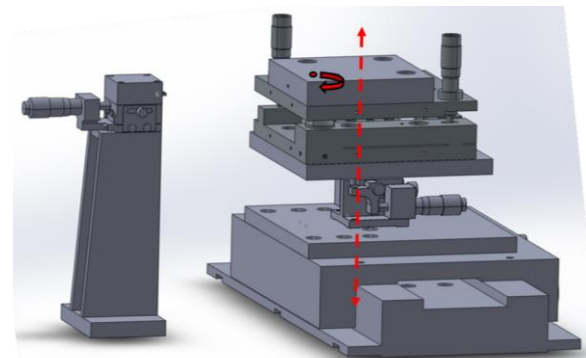


FIGURE 5. Vertical and rotational stage motions along and around z-axis for the lateral configuration.

As shown in Fig. 6 for the axial configuration, the highest slope on each plot was identified by fitting a line to the voltage-position curve, where the voltage was recorded in steps of 0.01 mm. The linear range was selected based on the value of the residual sum of squares from the fit. A maximum value of 0.05 was allowed. The slope of each linear range was then calculated. A higher slope indicates increased sensitivity. Figure 7 shows a voltage-position curve from the lateral configuration recorded in steps of 0.01 mm. It is observed that the voltage-displacement response is linear over the full range of the bipolar sensor for configuration B from Fig. 2.

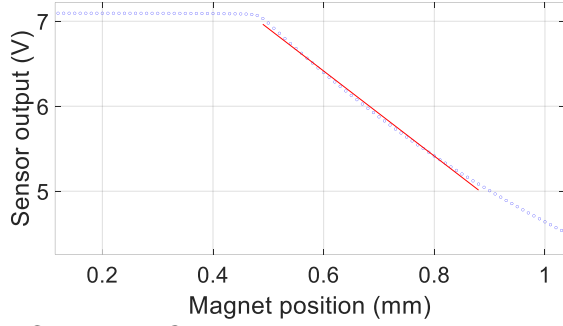


FIGURE 6. Change in voltage with magnet position (set by the air bearing stage position) for the axial configuration (see Fig. 1A). An N52 magnet and Texas Instruments 5056A1 unipolar sensor were used. The slope is 5 V/mm over a linear range of 0.39 mm (the red line identifies the fit). The residual sum of squares is 0.0481.

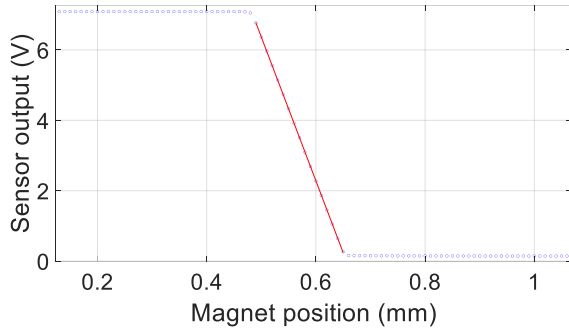


FIGURE 7. Change in voltage with magnet position (set by the air bearing stage position) for the lateral configuration (see Fig. 2B). Two N52 magnets and Texas Instruments 5055A1 bipolar sensor were used. The slope is 40.86 V/mm over a linear range of 0.16 mm (the red line identifies the fit). The residual sum of squares is 0.0013.

A comparison of results for the axial and lateral sensor-magnet configurations is provided in Figs. 8 and 9, where it is observed that the configurations with higher slopes have smaller linear ranges. The comparison was performed with different magnets and sensors to see their effects on the slope and linear range.

Tables 1 and 2 summarize the magnetic sensitivities and sensing ranges for the analog unipolar and bipolar Hall effect sensors. Table 3 shows the properties of the Neodymium magnets.

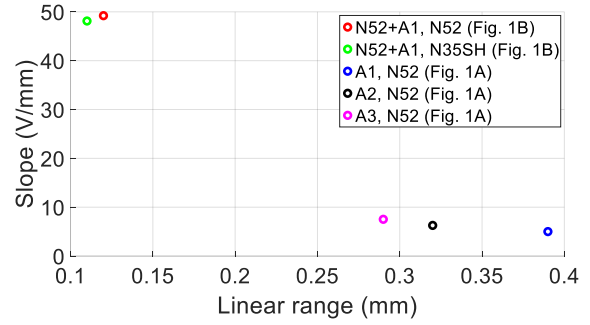


FIGURE 8. Slopes and linear ranges for the axial configuration using five sensor-magnet combinations. A1, A2, and A3 represent three Texas Instruments unipolar Hall effect sensors, while N52 and N35SH Neodymium magnets were used.

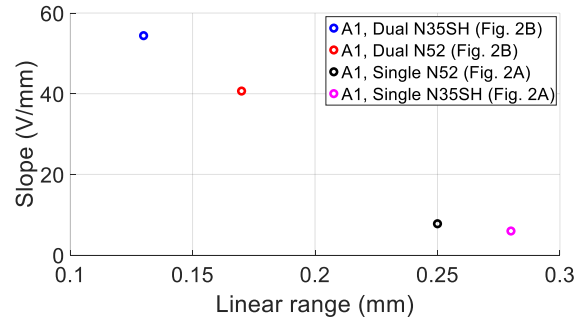


FIGURE 9. Slopes and linear ranges for the lateral configuration using four sensor magnet combinations. A1 represents a Texas Instruments bipolar Hall effect sensor.

TABLE 1. Unipolar Hall effect sensors.

Sensor (Texas Instruments)	Magnetic sensitivity (mV/mT at 5V)	Sensing range (\pm mT)
5056A1	200	20
5056A2	100	39
5056A3	50	79

TABLE 2. Bipolar Hall effect sensor.

Sensor (Texas Instruments)	Magnetic sensitivity (mV/mT at 5V)	Sensing range (\pm mT)
5055A1	100	21

TABLE 3. Neodymium magnets.

Magnet	Force (N)	Flux density (mT)	Dia. (mm)	Thickness (mm)
N52	0.445	1480	1.60	1.60
N35SH	2.669	1230	1.52	3.18

To evaluate the variation in sensitivity and linear range with misalignments between the magnet(s) and sensor, tests were performed as shown in Fig. 6 and 7 as the alignment was changed. The rotation and translation misalignment results are shown in Figs. 10 to 13. Three repeated tests were performed for each misalignment to determine repeatability. The rotation misalignments were applied in 0.03 deg and 0.06 deg steps, while the translation misalignments were applied in 0.05 mm and 0.1 mm steps. The zero location for each horizontal axis indicates the best visible alignment for the magnet-sensor configuration.

For each plot, the yellow regions identify the range of misalignments that were qualitatively too small to be visible to the physical eye. For the axial configuration (Figs. 10 and 11), the Texas Instruments unipolar sensor 5056A1 and two N52 magnets were used as shown in Fig. 1B. For the lateral configuration plots (Figs. 12 and 13), the Texas Instruments bipolar sensor 5055A1 and two N52 magnets were used as shown in Fig. 2B. The location of the center of rotation for the manual stage C used for rotation misalignments impacted the symmetry of the rotation sensitivity plots shown in Figs. 11 and 13 because the center of rotation was not located at the magnet face (see Fig. 4). As seen in Figs. 12 and 13, the lateral configuration demonstrates a larger change in slope with misalignment than the axial configuration.

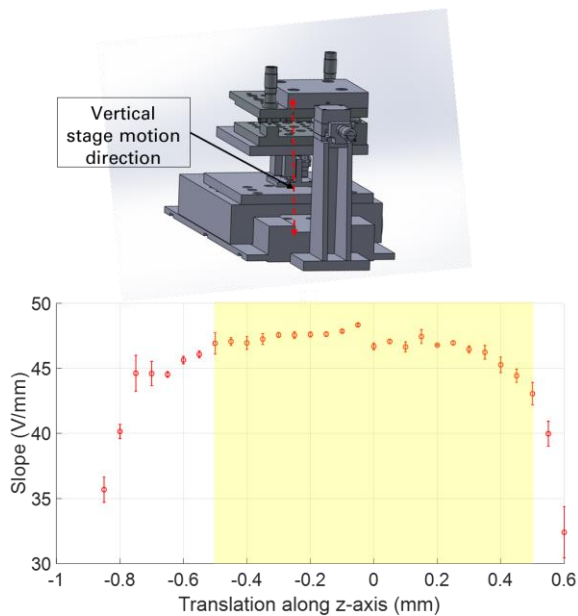


FIGURE 10. A schematic diagram and plot showing the axial configuration translation misalignments with error bars.

misalignments with error bars (± 1 standard deviation from repeated tests).

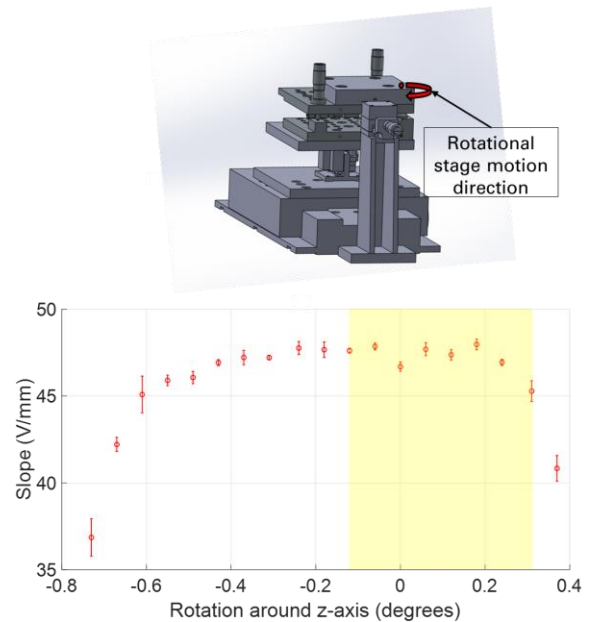


FIGURE 11. A schematic diagram and plot showing the axial configuration rotation misalignments with error bars.

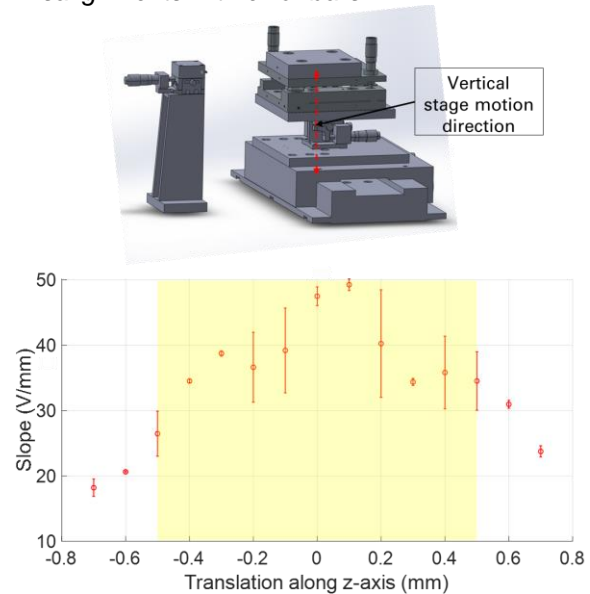


FIGURE 12. A schematic diagram and plot showing the lateral configuration translation misalignments with error bars.

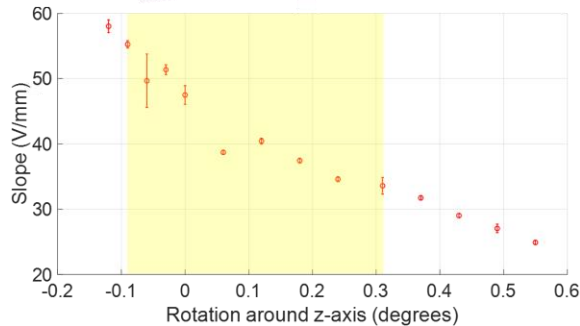
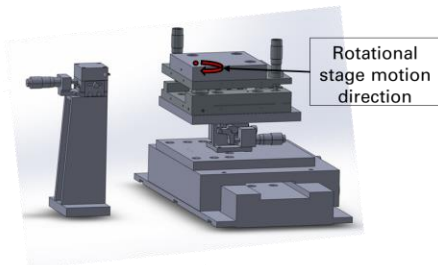


FIGURE 13. A schematic diagram and plot showing the lateral configuration rotation misalignments with error bars.

In Fig. 13, it would appear that a negative rotation misalignment from the nominal zero location is desired. While the slope does increase, the linear range subsequently decreases. The variations in linear range with misalignment is provided in Table 4.

TABLE 4. Variation in linear range with rotation misalignment for lateral configuration and three repetitions (Fig. 13).

Misalignment angle (degrees)	Linear range 1 (mm)	Linear range 2 (mm)	Linear range 3 (mm)
-0.12	0.10	0.10	0.10
-0.09	0.11	0.11	0.11
-0.06	0.14	0.12	0.12
-0.03	0.11	0.13	0.12
0.00	0.13	0.13	0.14
0.06	0.17	0.16	0.16
0.12	0.16	0.16	0.16
0.18	0.17	0.17	0.16
0.24	0.19	0.19	0.19
0.31	0.20	0.18	0.19
0.37	0.20	0.20	0.20
0.43	0.21	0.22	0.22
0.49	0.24	0.25	0.23
0.55	0.26	0.26	0.26

CONCLUSIONS

Tests were performed using combinations of Hall effect sensors and magnets in two primary

configurations: magnet motion along the sensor axis (axial) and magnet motion perpendicular to the sensor axis (lateral). The variation in the sensitivity and range with misalignment between the magnet(s) and sensor was measured. It was determined that the Hall effect sensor-magnet combination provides a viable low-cost displacement sensor.

ACKNOWLEDGEMENTS

The authors acknowledge support from the NSF Engineering Research Center for Hybrid Autonomous Manufacturing Moving from Evolution to Revolution (ERC-HAMMER) under Award Number EEC2133630.

REFERENCES

- [1] Yang, S.M. and Huang, C.L., 2009. A Hall sensor-based three-dimensional displacement measurement system for miniature magnetically levitated rotor. *IEEE Sensors Journal*, 9(12), pp.1872-1878.
- [2] Zhang, X., Mehrtash, M. and Khamesee, M.B., 2015. Dual-axial motion control of a magnetic levitation system using Hall-effect sensors. *IEEE/ASME Transactions on Mechatronics*, 21(2), pp.1129-1139.
- [3] Zhao, B., Wang, L. and Tan, J.B., 2015. Design and realization of a three degrees of freedom displacement measurement system composed of hall sensors based on magnetic field fitting by an elliptic function. *Sensors*, 15(9), pp.22530-22546.
- [4] Yarıçi, I. and Öztürk, Y., 2023. A new approach to linear displacement measurements based on Hall effect sensors. *Turkish Journal of Electrical Engineering and Computer Sciences*, 31(1), pp.238-248.
- [5] Lattanzi, E., Capellacci, P. and Freschi, V., 2023. A Machine Learning Enabled Hall-Effect IoT-System for Monitoring Building Vibrations. *International Journal of Advanced Computer Science and Applications*, 14(2).